

# An analytical stability theory for Faraday waves and the observation of the harmonic surface response

H. W. Müller†, H. Wittmer†, C. Wagner‡, J. Albers‡, K. Knorr‡

†*Institut für Theoretische Physik, Universität des Saarlandes, Postfach 151150, D 66041  
Saarbrücken, Germany*

‡*Institut für Technische Physik, Universität des Saarlandes, Postfach 151150, D 66041  
Saarbrücken, Germany*

## Abstract

We present an analytical stability theory for the onset of the Faraday instability, applying over a wide frequency range between shallow water gravity and deep water capillary waves. For sufficiently thin fluid layers the surface is predicted to occur in harmonic rather than subharmonic resonance with the forcing. An experimental confirmation of this result is given.

PACS: 47.20.Ma, 47.20.Gv, 47.15.Cb

The observation of standing waves at the surface of a fluid layer subjected to a vertical sinusoidal vibration dates back to Faraday [1]. For sufficiently strong forcing the plane surface undergoes an instability giving rise to ordered patterns of different orientational order [2–4]. For purely sinusoidal forcing spatially periodic patterns of lines, squares [5,6], hexagons and triangles [7] have been found, even quasiperiodic structures of 8-fold orientational order have been observed [8]. Faraday already recognized that the response of the surface appears with twice the period of the forcing. The first theoretical investigation of the linear stability [9] showed that the problem can be reduced to a set of Mathieu oscillators (parametrically driven pendula). However, the analysis takes advantage of the potential flow approximation which strictly applies to ideal (=inviscid) fluids only. Viscous effects are usually treated by introducing a heuristic damping term in the Mathieu equations [10] being proportional to the kinematic viscosity  $\nu$ . Its strength is estimated by evaluating the viscous energy dissipation in the bulk of the fluid. This approximation ignores viscous boundary layers which appear close to the borders of the fluid. Within these boundary layers the potential flow assumption breaks down giving rise to vortical flow, associated with additional damping. Kumar and Tuckerman [11] were the first who performed a linear stability analysis based on the viscid hydrodynamic field equations. Their fully numerical analysis uses Hill’s infinite determinant [12] and allows to approximate the critical quantities with any desired accuracy. They pointed out that the stability problem for viscous fluids cannot rigorously be reduced to a damped Mathieu oscillator. Beyer and Friedrich [13] demonstrated that a systematic treatment of the viscosity gives rise to a memory term in the Mathieu equation leading to an integro-differential equation. The integral gives rise to additional damping scaling – unlike bulk damping – with  $\nu^{3/2}$ . Since Beyer and Friedrich used idealized free slip boundary conditions they did not catch damping in the bottom boundary layer, which becomes crucial – as we shall see – for small filling depths. Recently Kumar [14] presented an approximative linear analysis based on a truncation of his numerical method [11]. For small damping he obtained an expression for the neutral stability curve, which requires a subsequent minimization with respect to the wave number to extract the threshold. Beside

of being rather implicit this approach is not systematic since one does not know to what order of viscosity the obtained result is valid [12]. Since damping strongly increases as the wavelength  $\lambda = 2\pi/k$  of the pattern compares to the filling depth  $h$ , Kumar [14] points out the possibility of observing the harmonic surface resonance rather than the subharmonic one. The necessary parameter combination is beyond of his analytical approach, that's why he provides an example by numerical means.

In the present paper we give a detailed account of the different damping mechanisms and develop a perturbative analytical treatment of the linear stability problem which does not suffer from the earlier shortcomings. We provide expressions for the critical onset acceleration  $a_c$  and the critical wave number  $k_c$  applying also to the case of shallow water waves ( $\lambda \simeq h$ ). The perturbation analysis is performed for the subharmonic (S) as well as for the harmonic (H) instability, allowing an easy prediction of the bicritical situation. Finally we present a Faraday experiment giving the first observation of surface waves in *harmonic* resonance with the forcing.

We consider a layer of an incompressible fluid of density  $\rho$ , depth  $h$  with a free upper surface in contact with air. The layer is subjected to a sinusoidal vertical vibration corresponding to a modulated gravitational acceleration  $g(t) = g_0 + a \cos 2\Omega t$  in the comoving frame of reference. Control parameters are the strength of the modulation  $a$  and the forcing frequency  $f = 2\Omega/(2\pi)$ . The free surface is initially flat at the vertical coordinate  $z = 0$ . As the forcing amplitude exceeds a critical threshold  $a_c$  the surface is located at the position  $z = \zeta(x, y, t)$ , where  $x, y$  are the horizontal coordinates and  $t$  is the time. For fluids of viscosity  $\nu$  and depth  $h$  the linear dispersion relation [14] for *free* (i.e.  $a = 0$ ) surface waves of the form  $\zeta \propto \exp i(kx - \omega t)$  is

$$0 = A(k, \omega) = \omega_0^2(k) + \frac{r(r^4 + 2r^2 + 5) \coth(rkh) - (1 + 6r^2 + r^4) \tanh(kh)}{r \coth(rkh) - \coth(kh)} \varepsilon^2 - \frac{4r(r^2 + 1) \tanh(kh) / (\cosh(kh) \cosh(rkh))}{r \coth(rkh) - \coth(kh)} \varepsilon^2, \quad (1)$$

with  $\omega_0^2(k) = \tanh(kh)[g_0k + (\sigma/\rho)k^3]/\Omega^2$ ,  $\varepsilon = \nu k^2/|\Omega|$  and  $r = \sqrt{1 + i\omega/\varepsilon}$ . The square root with the positive real part is assumed. To shorten notation we have nondimensionalized time  $t$  and frequencies  $\omega$ ,  $\omega_0$  by the control parameter  $\Omega$ . In the ideal fluid limit  $\nu \rightarrow 0$  Eq. 1 reduces to the well known gravity-capillary dispersion relation  $\omega^2 = \omega_0^2(k)$ . The periodic forcing is introduced by replacing  $g_0$  in  $\omega_0^2$  by  $g(t)$ . This parametric driving couples different temporal Fourier modes and the following linear evolution equation for the Fourier transform  $\hat{\zeta}(\omega) = \int \exp(-i\omega t) \zeta(t) dt$  of the surface elevation results

$$A(k, \omega) \hat{\zeta}(\omega) + \frac{a k \tanh(kh)}{2\Omega^2} [\hat{\zeta}(\omega - 2) + \hat{\zeta}(\omega + 2)] = 0. \quad (2)$$

It is useful to account for the different length scales of relevance in the Faraday experiment (see Fig. 1). Intrinsic are the wavelength  $\lambda = 2\pi/k$  of the surface pattern, the thickness of the viscous boundary layer  $\delta = \sqrt{2\nu/|\Omega|}$ , and the capillary length  $\sqrt{\sigma/(\rho g_0)}$ , where  $\sigma$  is the surface tension. Dictated by the geometry are the filling depth  $h$  and the lateral dimension of the vessel  $L$ , which we ignore here by assuming  $L \rightarrow \infty$ .

In order to make analytical progress we confine ourselves to the limit of low viscosity  $\varepsilon \ll 1$ , telling that the depth of the viscous boundary layer is small compared to the wavelength. Furthermore we assume that  $h$  is at least a few times larger than the thickness of the viscous boundary layer,  $h/\sqrt{2\nu/|\Omega|} \gtrsim 3$ , giving  $\coth(rkh) \simeq 1$  and  $1/\cosh(rkh) \simeq 0$ . Note that there is no restriction upon the relation between  $h$  and  $\lambda$ . The two simplifications made are not very restrictive and include almost all recent experiments. Even in the measurements of Edwards and Fauve [6] with a high viscosity water-glycerol mixture  $\varepsilon$  did not exceed a value of 0.4. We first expand Eq. 1 in powers of  $1/r = O(\sqrt{\varepsilon})$  giving

$$A(k, \omega) = \omega_0^2 - \omega^2 + i\omega\varepsilon(3 + \coth^2) + \frac{\varepsilon^{1/2}\sqrt{\varepsilon + i\omega}^3}{\sinh \cosh} + \varepsilon^{3/2}\sqrt{\varepsilon + i\omega}(-6 \tanh + \coth + \coth^3) + \dots, \quad (3)$$

where we have abbreviated  $\coth(kh)$  by  $\coth$  *etc.* This formulation is particularly useful for a physical interpretation. Transformation of Eq. 3 into real space yields a damped Mathieu oscillator with integral contributions [15]

$$\begin{aligned}
0 = & \ddot{\zeta}(t) + \varepsilon(3 + \coth^2)\dot{\zeta}(t) + \left[ \omega_0^2 + \frac{a k \tanh}{\Omega^2} \cos(2t) \right] \zeta(t) + \\
& \frac{\varepsilon^{1/2}}{\sqrt{\pi} \sinh \cosh} \int_{-\infty}^t G(t - \tau) (\varepsilon + \partial_\tau)^2 \zeta(\tau) d\tau + \\
& \frac{-6 \tanh + \coth + \coth^3}{\sqrt{\pi}} \varepsilon^{3/2} \int_{-\infty}^t G(t - \tau) (\varepsilon + \partial_\tau) \zeta(\tau) d\tau,
\end{aligned} \tag{4}$$

where  $G(t) = \exp(-\varepsilon t)/\sqrt{t}$ . Beside the usual (bulk) damping ( $\propto \dot{\zeta}$ ) the two integrals also contribute to the dissipation. This nonlocal temporal behavior is analogous to the propagation of thermal waves into a medium which is heated at its boundary. Here, the moving surface emits velocity waves into the interior of the fluid giving rise to dissipation which depends on the history of  $\zeta(t)$ . The first memory integral scales like  $O(\nu^{1/2})$  and governs the expansion in the shallow water limit  $kh = O(1)$ . It is associated with damping in the bottom boundary layer and dies out exponentially ( $1/(\sinh kh \cosh kh)$ ) as  $kh$  increases. The second integral (c.f. Ref. [13]) survives for  $h \rightarrow \infty$ . It scales with  $\nu^{3/2}$  and is related to the dissipation within the surface boundary layer.

To proceed with the linear stability analysis we reexpand the square roots in Eq. 3 giving

$$A(k, \omega) = -\omega^2 + X(k, \omega) + \omega_0^2, \tag{5}$$

where all viscous contributions up to  $O(\varepsilon^{3/2})$  are collected in

$$\begin{aligned}
X(k, \omega) = & \Re(X) + i \Im(X) = \\
& -\varepsilon^{1/2} \frac{|\omega|^{3/2}}{\sqrt{2} \sinh \cosh} + \varepsilon^{3/2} \frac{|\omega|^{1/2}}{2\sqrt{2}} (-15 \tanh + 5 \coth + 2 \coth^3) + \\
& i \operatorname{sgn}(\omega) \left[ \varepsilon^{1/2} \frac{|\omega|^{3/2}}{\sqrt{2} \sinh \cosh} + \varepsilon |\omega| (3 + \coth^2) + \varepsilon^{3/2} \frac{|\omega|^{1/2}}{2\sqrt{2}} (-15 \tanh + 5 \coth + 2 \coth^3) \right]. \tag{6}
\end{aligned}$$

We first investigate the subharmonic resonance of the surface elevation by introducing

$$\hat{\zeta}(\omega) = \alpha_1 \delta(\omega - 1) + \alpha_2 \delta(\omega + 1) + \hat{\zeta}_1 + \dots \tag{7}$$

in Eq. 2. Assuming a small detuning  $\omega_0^2 - 1 = O(X)$  the solvability condition for  $\hat{\zeta}_1 = O(X)$  yields the neutral stability curve

$$\left[ X(k, 1) + (\omega_0^2 - 1) \right] \left[ X(k, -1) + (\omega_0^2 - 1) \right] = \left( \frac{a k \tanh}{2\Omega^2} \right)^2. \quad (8)$$

The minimum of the forcing amplitude  $a$  with respect to  $\omega_0^2$  [16] relates the onset of the subharmonic response to the imaginary part of  $X$

$$a_c^{(S)} \simeq \frac{2\Omega^2}{k_S} \coth(kh) \Im [X(k_S, 1)], \quad (9)$$

while the critical wave number  $k_S$  results from the dispersion relation corrected by the real part

$$\omega_0^2(k_S) \simeq 1 - \Re [X(k_S, 1)]. \quad (10)$$

For a typical experimental situation Fig. 2 compares our analytical formula Eq. 9 with the full numerical computation according to the method of Kumar and Tuckerman [11]. Excellent agreement is achieved over a wide frequency range between shallow water gravity and deep water capillary waves. The three contributions in  $\Im(X)$  (Eq. 6) are respectively related to damping in the bottom boundary layer, the bulk, and the surface boundary layer, which become important at low, intermediate, and higher forcing frequencies. Even the sharp reincrease of the onset amplitude at low frequencies (shallow water limit  $kh \simeq 1$ ) is well reproduced. Consistence of the perturbation expansion up to  $O(\varepsilon^{3/2})$  requires  $1/(\sinh \cosh) \leq O(\varepsilon^{1/2})$ , which reflects a low frequency limit for the validity of Eqs. 9,10. At high excitation frequencies  $\Omega$  the validity is limited by the size of the expansion coefficient  $\varepsilon$ .

A similar perturbation expansion can be computed for the first *harmonic* stability tongue. We obtain for the onset amplitude

$$a_c^{(H)} \simeq \frac{4\Omega^2}{k_H} \coth(k_H h) \sqrt{\Im [X(k_H, 2)]} \quad (11)$$

with the critical wave number  $k_H$  determined by

$$\omega_0^2(k_H) \simeq 4 + \frac{2}{3} \Im [X(k_H, 2)] - \Re [X(k_H, 2)]. \quad (12)$$

A comparison with the exact numerical stability analysis (Fig. 2) shows that the agreement is worse than for the subharmonic response. The sharp increase of  $a_c^{(S)}$  at low frequencies leads to an intersection with  $a_c^{(H)}$  and thus to a situation where the harmonic response preempts the subharmonic one. This phenomenon, however, is difficult to observe experimentally: The corresponding  $\Omega$ -window is rather narrow as it is also limited from below by the *second* subharmonic resonance (see Ref. [14]). An additional problem is a technical one and applies to most of the commercial shaker systems being in use for Faraday experiments: For the considered excitation frequencies ( $f \simeq 10Hz$ ) it is usually the maximum peak *elevation* (but not the maximum *force*) which prevents the apparatus from reaching the threshold amplitude  $a_c^{(H)}$ .

In order to observe the harmonic surface resonance we set up a Faraday experiment. We used a cylindrical aluminum container of radius  $R = 45mm$  and depth  $h = 5mm$ . Between  $R = 35mm$  and the outer edge the depth continuously decreases to zero. This provides increasing damping in order to suppress meniscus waves. Working fluid is a silicone oil (Dow Corning 200) with a viscosity of  $8.9mm^2/s$ , surface tension of  $19.8 \star 10^{-3}N/m$ , and density of  $0.929g/cm^3$  at a temperature  $T = 30^\circ C$ . We use an electromagnetic shaker V400 (LDS) with a maximum force of  $98N$  and an indicated maximum peak elevation of 8 mm. Waveform generation as well as data acquisition is performed by a PC. The acceleration is measured by a piezoelectric device (Bruel and Kjaer 4393). For pattern visualization the container is lighted from the top by a concentric ring (20cm in diameter) of 50 high intensity light emitting diodes (LED) allowing for a stroboscopic illumination. A CCD camera located in the middle of the ring observes the pattern from the top. The LED's are synchronized to the forcing and triggered by either the same or twice the excitation period. Duty cycle as well as the relative phase of the illumination with respect to the forcing can be controlled externally. This technique allows a clear distinction between the subharmonic and harmonic surface resonance. As explained earlier bottom damping plays a crucial role for the appearance of the harmonic Faraday instability; thus a depth to wavelength ratio of  $kh \lesssim 1$  is required. For practical purposes filling depths much less than a millimeter are unsuitable

and difficult to control, we used  $h \simeq 0.8\text{mm}$ . For this parameter combination the stability theory predicts the harmonic-subharmonic bicriticality,  $a_c^{(S)} = a_c^{(H)}$ , at  $f \simeq 9\text{Hz}$ , which is close to the low frequency limit of our apparatus. Fig. 3a presents a photograph of a pattern in harmonic resonance with the forcing. Both, the vessel and the surface were oscillating synchronously with  $9\text{Hz}$ . To confirm our observation we show in Fig. 3b a subharmonic surface pattern, oscillating again with  $9\text{Hz}$  but excited with  $f = 18\text{Hz}$ . As expected, the wavelength in Fig. 3a and b are the same. Finally Fig. 3c depicts a subharmonic pattern driven at  $f = 10\text{Hz}$  exhibiting a considerably larger wavelength. All patterns are achieved by slowly increasing the forcing amplitude  $a$  beyond the threshold while keeping  $f$  constant. The small aspect ratio of our container (diameter to wavelength ratio) did not allow the observation of nice ordered structures. Thus redoing the experiment with a larger (and thus heavier) container would indeed be desirable, however, exceeds the specifications of our shaker [17].

In summary we have presented an analytical theory for the onset of the Faraday instability. The analysis is based on the low viscosity approximation and assumes a filling depth larger than the thickness of the viscous boundary layer. Almost all recent experiments are covered by these assumptions. Particularly interesting is the case of shallow water waves ( $\lambda \simeq h$ ) for which the harmonic instability preempts the subharmonic one. This theoretical prediction is confirmed by an experiment.

*Acknowledgements* — Fruitful discussions with S. Fauve are gratefully acknowledged. This work is supported by the Deutsche Forschungsgemeinschaft.



## REFERENCES

- [1] M. Faraday, Philos. Trans. R. Soc. London **52**, 319 (1831).
- [2] N. B. Tuffillaro, R. Ramshankar, and J. P. Gollub, Phys. Rev. Lett. **62**, 422 (1989).
- [3] J. W. Miles and D. Henderson, Ann. Rev. Fluid Mech. **22**, 143 (1990).
- [4] J. P. Gollub, Physica D **51**, 501 (1991).
- [5] S. Douady, J. Fluid Mech. **221**, 383 (1990).
- [6] W. S. Edwards und S. Fauve, J. Fluid Mech. **278**, 123 (1994).
- [7] K. Kumar, K. M. Bajaj, Phys. Rev. E **52**, R4606 (1995).
- [8] B. Christiansen, P. Alstrom und M. T. Levinsen, Phys. Rev. Lett. **68**, 2157 (1992).
- [9] T. B. Benjamin und F. Ursell, Proc. R. Soc. Lond. A **225** 505 (1954).
- [10] L. Landau and E. M. Lifshitz, Fluid Mechanics, 2nd edn. Pergamon Press (1987).
- [11] K. Kumar und L. S. Tuckerman, J. Fluid Mech. **279** 49 (1994).
- [12] A. H. Nayfeh and D. T. Mook, *Nonlinear oscillations*, Wiley (1979).
- [13] J. Beyer and R. Friedrich, Phys. Rev. E **51**, 1162 (1995).
- [14] K. Kumar, Proc. R. Soc. Lond. A **452**, 1113 (1996).
- [15] to transform  $\sqrt{\varepsilon + i\omega}$  and  $\sqrt{\varepsilon + i\omega}^3$  into time space use the identity  

$$1/\sqrt{\pi} \int_0^\infty u^{-1/2} \exp[-(\varepsilon + i\omega)u] du = (\varepsilon + i\omega)^{-1/2}.$$
- [16] Up to  $O(X)$  minimization with respect to  $k$  and  $\omega_0^2$  are equivalent.
- [17] To obtain the harmonic surface resonance (Fig.3a) we already exceeded the maximum elevation of our shaker by 50% generating a slightly imperfect sinusoidal excitation. However, the second harmonic contribution to the vessel vibration was less than 2% of the amplitude of the 9Hz-basic forcing frequency.

## FIGURES

FIG. 1. Length scales of relevance: Wavelength of the pattern  $\lambda = 2\pi/k$ , thickness of the viscous boundary layers  $\delta = \sqrt{2\nu/\Omega}$ , depth of the layer  $h$ , and lateral extension of the container  $L$ . Energy dissipation in the various regions scales with different powers of the viscosity  $\nu$  (exponents are indicated in paranthesis). Waves with a wavelength larger (smaller) than the capillary length  $\rho g_0/\sigma$  (not shown in the figure) are called gravity (capillary) waves.

FIG. 2. The critical onset amplitude for the subharmonic (S) and harmonic (H) Faraday instability as a function of the forcing frequency  $f = \Omega/\pi$ . Solid lines correspond to the analytical results (Eqs.9 and 11), dashed lines are obtained by an exact numerical treatment. At low forcing frequencies the harmonic instability preempts the subharmonic one. Parameters:  $\rho = 0.934g/cm^3$ ,  $\sigma = 20.1 \star 10^{-3}N/m$ ,  $\nu = 10mm^2/s$ ,  $h = 1mm$ .

FIG. 3. Surface patterns as observed in the experiment. (a): Driving force and surface oscillate synchronously at  $f = 9Hz$  (harmonic response). ; (b) Subharmonic surface response with  $9Hz$  at a forcing with  $f = 18Hz$ ; (c) Subharmonic surface oscillation with  $5Hz$  at a forcing with  $f = 10Hz$ .

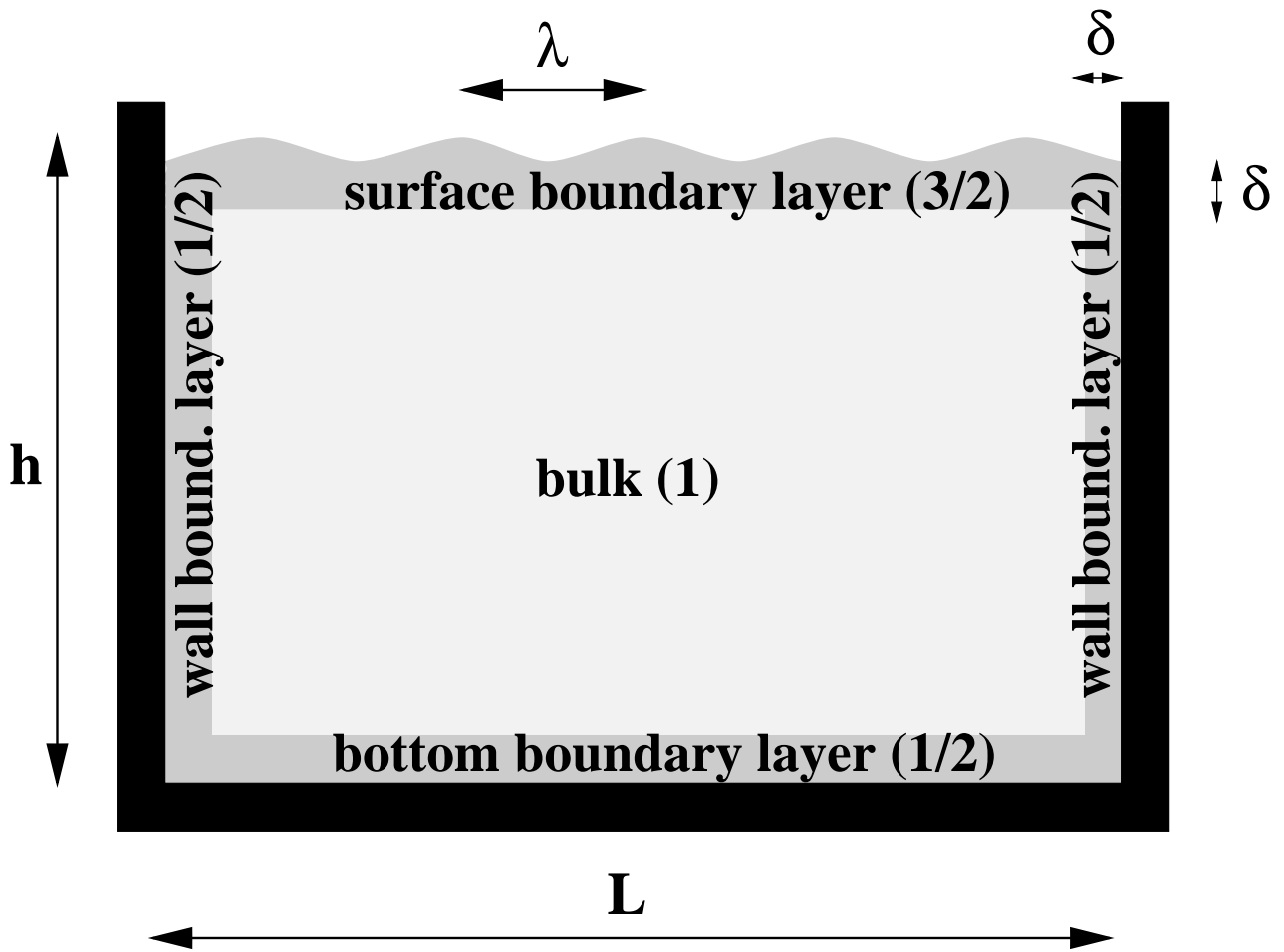
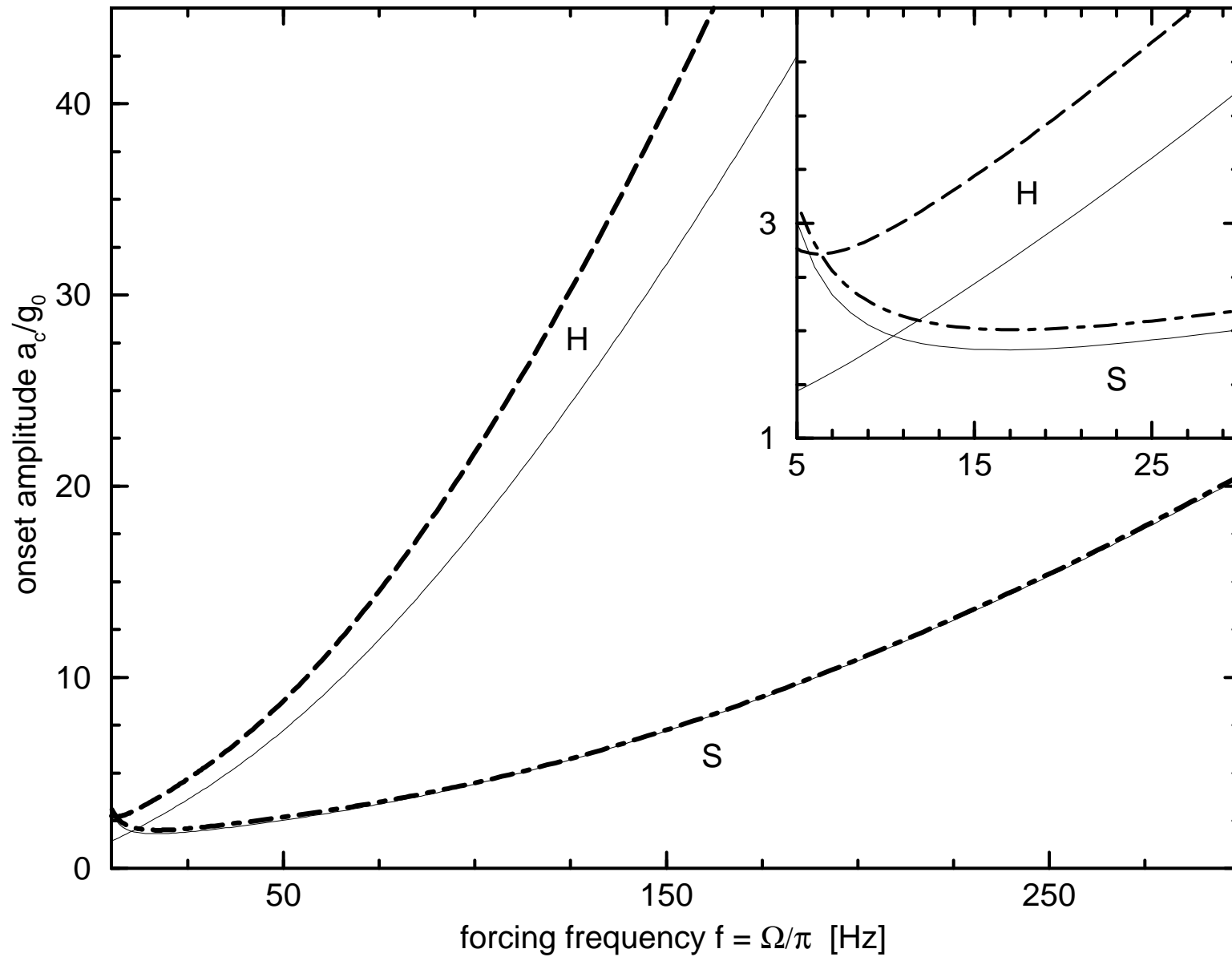


Fig.1: An analytical stability theory for Faraday waves ...  
by Muller et al.

Fig.2: An analytical stability theory for Faraday waves ...

by Muller et al.



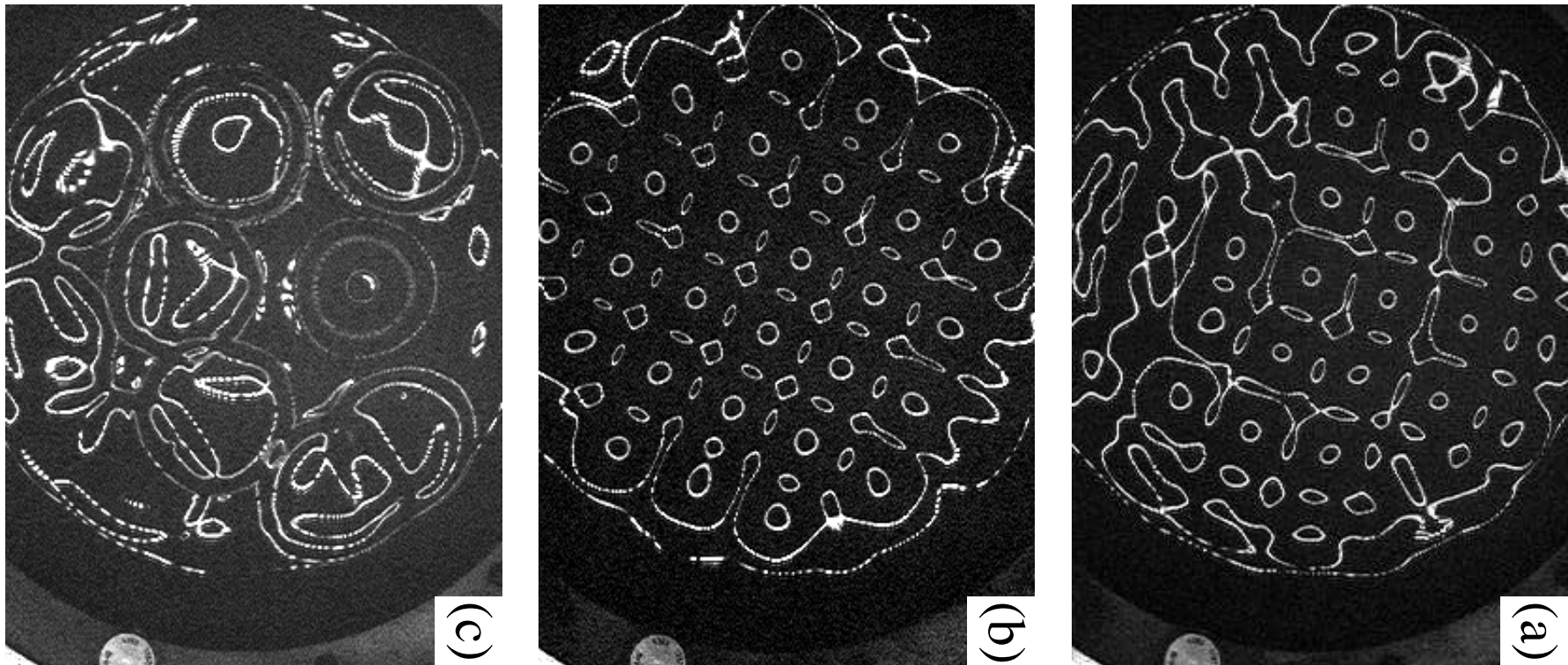


Fig.3: An analytical stability theory for Faraday waves ...  
by Muller et al.